Inherent and apparent scattering properties of coated or uncoated spheres embedded in an absorbing host medium

Ping Yang, Bo-Cai Gao, Warren J. Wiscombe, Michael I. Mishchenko, Steven E. Platnick, Hung-Lung Huang, Bryan A. Baum, Yong X. Hu, Dave M. Winker, Si-Chee Tsay, and Seon K. Park

The conventional Lorenz–Mie formalism is extended to the case for a coated sphere embedded in an absorbing medium. The apparent and inherent scattering cross sections of a particle, derived from the far field and near field, respectively, are different if the host medium is absorptive. The effect of absorption within the host medium on the phase-matrix elements associated with polarization depends on the dielectric properties of the scattering particle. For the specific cases of a soot particle coated with a water layer and an ice sphere containing an air bubble, the phase-matrix elements $-P_{12}/P_{11}$ and P_{33}/P_{11} are unique if the shell is thin. The radiative transfer equation for a multidisperse particle system embedded within an absorbing medium is discussed. Conventional multiple-scattering computational algorithms can be applied if scaled apparent single-scattering properties are applied.

OCIS codes: 010.1290, 010.1310, 010.3920, 290.5850, 290.1090, 280.1310.

1. Introduction

The geometric shapes of many micrometer-sized natural particles including cloud droplets can be well approximated as spheres in light-scattering calculations. The Lorenz–Mie theory[1] provides the theoretical basis for studying the interaction between a sphere and an electromagnetic wave (e.g., Refs. 2–5). Numerically stable and efficient algorithms and the corresponding computational codes have been developed[4–8] to derive the exact single-scattering properties of spherical particles. Although the scattering problem associated with spheres, involved in many applications including aircraft and satellite remote sensing, seems to be solved, an issue on this subject still needs to be addressed. In the conventional Lorenz–Mie formulation, the host medium within which the sphere is embedded is assumed to be a nonabsorptive dielectric material such as air. For many situations, the medium surrounding the spherical particles may contain constituents with significant absorption. For example, ozone and CO_2 in the atmosphere have strong absorptive bands at 9.6 and 15 μm, respectively. In addition, atmospheric water vapor provides a strongly absorbing component to the air surrounding spherical aerosol or water particles in both solar and infrared spectral regions.

For scattering of solar and infrared radiation by atmospheric particles embedded in an absorbing medium, the absorption effect of the host medium on the scattering properties of the particles may not be negligible. When the host medium is transparent (i.e., a dielectric medium with a purely real refractive index), use of the standard Lorenz–Mie formulation

P. Yang (pyang@ariel.met.tamu.edu) is with the Department of Atmospheric Sciences, Texas A&M University, 3150 TAMU, College Station, Texas 77843. B.-C. Gao is with the Remote Sensing Division, Code 7212, U.S. Naval Research Laboratory, Washington, D.C. 20375. W. J. Wiscombe, S. E. Platnick, and S.-C. Tsay are with NASA Goddard Space Flight Center, Code 913, Greenbelt, Maryland 20771. M. I. Mishchenko is with NASA Goddard Institute for Space Studies, 2880 Broadway, New York, New York 10025. H.-L. Huang is with the Cooperative Institute for Meteorological Satellite Studies, University of Wisconsin-Madison, 1225 West Dayton Street, Madison, Wisconsin 53706. B. A. Baum, (bryan.baum@ssec.wisc.edu) Y. X. Hu, and D. M. Winker are with the Atmospheric Sciences Division, Mailstop 420, NASA Langley Research Center, Hampton, Virginia 23681. S. K. Park is with the Department of Environmental Sciences and Engineering, Ewha Women's University, Seoul 120-750, Republic of Korea.

Received 25 July 2001, revised manuscript received 07 December 2001.

0003-6935/02/152740-20$15.00/0

does not raise any difficulty. In this case, the effect of the host medium can be accounted for by a determination of a relative refractive index for the scattering particle, which is defined as the ratio of the particle refractive index to that of its host counterpart. Unfortunately, one cannot obtain the scattering properties of a sphere in an absorbing medium by simply modifying the refractive indices for the particle and the host medium along with scaling the incident wavelength in the input list of the conventional Mie computational code. Thus there is a necessity to reformulate the conventional Lorenz–Mie theory to accommodate a spherical particle embedded in an absorbing medium.

The scattering properties of a homogeneous sphere in an absorbing medium have been investigated by several authors.[9–12] On this specific issue, two approaches that are based either on the asymptotic form of the electromagnetic field in the radiation zone (i.e., the far field)[9] or on the information of the field at the particle surface (i.e., the near field)[11,12] have been used in the previous calculation of the extinction and scattering cross sections. When the host medium is absorptive, the host absorption has not only attenuated the scattered wave in magnitude but also modulated the wave mode when the wave reaches the radiation zone. Thus, for an observation in the radiation zone, the particle's inherent optical properties are coupled with the absorption effect of the medium in an inseparable manner. For this reason, the scattering properties of the particle that are derived from the far-field asymptotic form of the scattered wave, although rescaled by removal of the exponential absorption of the host medium between the particle and the observational point, are the apparent optical properties of the scattering particle. The apparent scattering and extinction cross sections for a sphere in an absorbing medium have been derived by Mundy *et al.*[9], which unfortunately may be implausible at times because the corresponding extinction efficiency can be smaller than the scattering efficiency. This discrepancy is caused when the absorption of the incident wave within the host medium is neglected in the calculation of the extinction cross section, as is shown by Chylek.[10] The true or inherent scattering and absorption cross sections of the particle can be calculated when the Poynting vector is integrated at the scattering particle's surface as shown by Chylek.[10] The apparent optical properties reduce to their corresponding inherent counterparts if the absorption of the host medium is absent. Most recently, Sudiarta and Chylek[11] reported the numerical calculations for the inherent extinction and scattering efficiencies based on the theoretical frame developed in Chylek's previous research.[10] Similar calculations were reported by Fu and Sun[12] who also investigated the effect of absorption within the host medium on the phase function and asymmetry factor.

The inherent extinction and scattering efficiencies have limited applications in practice for three reasons. First, these efficiencies do not have the conventional meanings in that the corresponding cross sections are not simply the products of these efficiencies and the geometric projected area of the particle. In fact, because the incident irradiance spatially varies when the host medium is absorptive, a reference plane must be specified to unambiguously define the extinction and scattering cross sections. Second, to consider the bulk scattering properties of a polydispersive system, one always deals with the far field and consequently the apparent optical properties. Third, the motivation to determine particle single-scattering properties is primarily for radiative transfer calculations that require both cross sections and an accurate description of the phase matrix. It is not self-consistent to use the inherent cross sections in radiative transfer calculations when the corresponding phase matrix is an apparent optical property.

The intent of this study is to properly define the apparent extinction and scattering cross sections versus their inherent counterparts. In addition, we also investigate the effect of host absorption on the polarization configuration of the scattered wave because the previous studies focused primarily on the total cross sections and scattered intensity. Furthermore, because the scattering properties of coated spheres such as black carbon aerosols that are coated with water are of interest in many disciplines including atmospheric remote sensing and radiative transfer calculations, we also present a solution for the scattering properties of a coated sphere in an absorbing host medium. The previous solution for a homogeneous sphere in an absorbing medium is a special case of the present study when the core and shell of the coated sphere have the same refractive index. In Section 2 we present the basic mathematical expressions for the inherent and apparent scattering properties of a coated sphere within an absorbing medium. In Section 2 we also discuss the proper form of the single-scattering properties for radiative transfer calculation involving a polydisperse particle system in an absorbing host medium. Presented in Section 3 are the numerical results and discussion. Finally, the conclusions are given in Section 4.

2. Inherent and Apparent Optical Properties of Coated Spheres in an Absorbing Medium

A. Transverse Components of Incident and Scattered Waves in a Spherical Coordinate System for Coated Spheres Embedded in an Absorbing Medium

In this study we select the time-dependent factor $\exp(-i\omega t)$ for the complex representation of a temporally harmonic electromagnetic wave, where ω is the angular frequency of the wave. In addition, we employ the Gaussian unit system for the electromagnetic field. Let us consider the scattering of an incident electromagnetic wave by a coated sphere embedded in an absorbing medium. As shown in Fig. 1, the complex refractive indices for the particle core, particle shell, and the host medium are m_1, m_2, and m_0, respectively. Let the incident electric field be polarized along the x axis and propagate along the z

axis of the coordinate system. Thus the incident electric and magnetic fields can be written as follows:

$$\mathbf{E}_i(x, y, z) = \hat{e}_x E_0 \exp(ikm_0 z), \tag{1a}$$

$$\mathbf{H}_i(x, y, z) = -\frac{i}{k} \nabla \times \mathbf{E}_i(x, y, z) = \hat{e}_y m_0 E_0 \exp(ikm_0 z), \tag{1b}$$

where $k = \omega/c$ in which c is the speed of light *in vacuo*; E_0 is the amplitude of the electric field; and $\hat{e}_x$ and $\hat{e}_y$ are the unit vectors along the x axis and y axis, respectively. Note that in the present study we assume permeability to be unity. The expansions of incident and scattering fields in terms of spherical harmonics for a coated sphere within an absorbing medium are similar to their counterparts in the case of the conventional Mie formulation. To derive inherent and apparent cross sections and the scattering phase matrix, it is sufficient to consider the transverse components of the incident and scattered fields decomposed in a spherical coordinate system. It can be shown that these field components can be expanded in the form

$$E_{i\theta}(\phi, \theta, r) = \frac{\cos\phi}{m_0 kr} \sum_{n=1}^{\infty} E_n[\pi_n(\cos\theta)\psi_n(m_0 kr) - i\tau_n(\cos\theta)\psi_n'(m_0 kr)], \tag{2a}$$

$$E_{i\phi}(\phi, \theta, r) = -\frac{\sin\phi}{m_0 kr} \sum_{n=1}^{\infty} E_n[\tau_n(\cos\theta)\psi_n(m_0 kr) - i\pi_n(\cos\theta)\psi_n'(m_0 kr)], \tag{2b}$$

$$H_{i\theta}(\phi, \theta, r) = \frac{\sin\phi}{kr} \sum_{n=1}^{\infty} E_n[\pi_n(\cos\theta)\psi_n(m_0 kr) - i\tau_n(\cos\theta)\psi_n'(m_0 kr)], \tag{2c}$$

$$H_{i\phi}(\phi, \theta, r) = \frac{\cos\phi}{kr} \sum_{n=1}^{\infty} E_n[\tau_n(\cos\theta)\psi_n(m_0 kr) - i\pi_n(\cos\theta)\psi_n'(m_0 kr)], \tag{2d}$$

$$E_{s\theta}(\phi, \theta, r) = \frac{\cos\phi}{m_0 kr} \sum_{n=1}^{\infty} E_n[ia_n\tau_n(\cos\theta)\xi_n'(m_0 kr) - b_n\pi_n(\cos\theta)\xi_n(m_0 kr)], \tag{2e}$$

$$E_{s\phi}(\phi, \theta, r) = -\frac{\sin\phi}{m_0 kr} \sum_{n=1}^{\infty} E_n[ia_n\pi_n(\cos\theta)\xi_n' \times (m_0 kr) - b_n\tau_n(\cos\theta)\xi_n(m_0 kr)], \tag{2f}$$

$$H_{s\theta}(\phi, \theta, r) = -\frac{\sin\phi}{kr} \sum_{n=1}^{\infty} E_n[a_n\pi_n(\cos\theta)\xi_n(m_0 kr) - ib_n\tau_n(\cos\theta)\xi_n'(m_0 kr)], \tag{2g}$$

$$H_{s\phi}(\phi, \theta, r) = -\frac{\cos\phi}{kr} \sum_{n=1}^{\infty} E_n[a_n\tau_n(\cos\theta)\xi_n(m_0 kr) - ib_n\pi_n(\cos\theta)\xi_n'(m_0 kr)], \tag{2h}$$

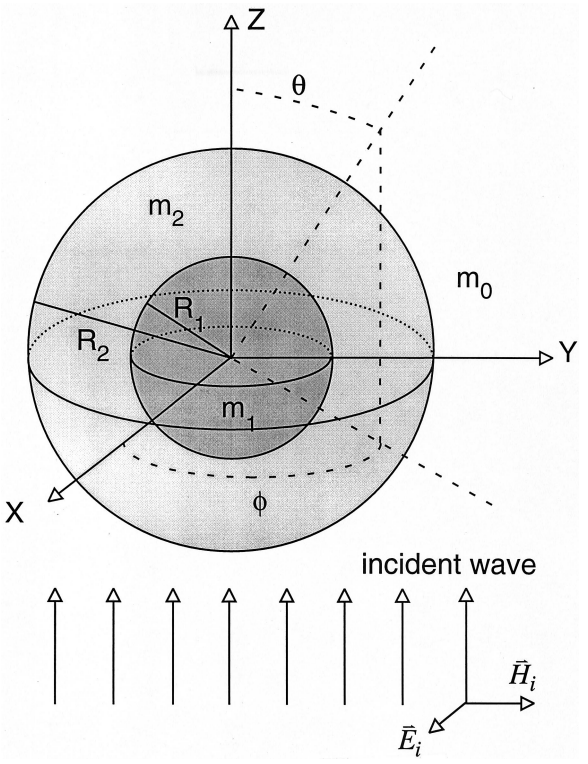

Fig. 1. Geometry for scattering by a coated sphere embedded in an absorbing medium.

where we employed the common nomenclature for the special functions involved in the Lorenz–Mie algorithm (e.g., Refs. 2, 4, 5); for example, ψ_n and ξ_n indicate Riccati–Bessel functions associated with the spherical Bessel function j_n and the Hankel function $h_n^{(1)}$, respectively. The functions π_n and τ_n are the functions of the scattering zenith angle and are related to the associated Legendre function P_n^1. The coefficient E_n can be determined from the orthogonality of the spherical harmonics and is given by

$$E_n = E_0 i^n (2n + 1)/[n(n + 1)]. \tag{3}$$

The coefficients a_n and b_n in Eqs. (2e)–(2h) for the scattered field can be determined from an electromagnetic boundary condition that is imposed at both the interfaces of the core and the shell of the particle and the interface of the scatterer and the host medium. Here, without a detailed derivation, we give these coefficients in a form similar to that presented in Bohren and Huffman[5] as follows:

$$a_n = \frac{[\tilde{D}_n m_0/m_2 + n/(m_0 kR_2)]\psi_n(m_0 kR_2) - \psi_{n-1}(m_0 kR_2)}{[\tilde{D}_n m_0/m_2 + n/(m_0 kR_2)]\xi_n(m_0 kR_2) - \xi_{n-1}(m_0 kR_2)}, \tag{4a}$$

$$b_n = \frac{[\tilde{G}_n m_2/m_0 + n/(m_0 kR_2)]\psi_n(m_0 kR_2) - \psi_{n-1}(m_0 kR_2)}{[\tilde{G}_n m_2/m_0 + n/(m_0 kR_2)]\xi_n(m_0 kR_2) - \xi_{n-1}(m_0 kR_2)}, \tag{4b}$$

$$\tilde{D}_n = \frac{D_n(m_2kR_2) - A_n[\chi_n'(m_2kR_2)/\psi_n(m_2kR_2)]}{1 - A_n[\chi_n(m_2kR_2)/\psi_n(m_2kR_2)]}, \tag{4c}$$

$$\tilde{G}_n = \frac{D_n(m_2kR_2) - B_n[\chi_n'(m_2kR_2)/\psi_n(m_2kR_2)]}{1 - B_n[\chi_n(m_2kR_2)/\psi_n(m_2kR_2)]}, \tag{4d}$$

$$A_n = \frac{m_2D_n(m_1kR_1) - m_1D_n(m_2kR_1)}{m_2D_n(m_1kR_1)\,[\chi_n(m_2kR_1)/\psi_n(m_2kR_1)] - m_1[\chi_n'(m_2kR_1)/\psi_n(m_2kR_1)]}, \tag{4e}$$

$$B_n = \frac{m_1D_n(m_1kR_1) - m_2D_n(m_2kR_1)}{m_1D_n(m_1kR_1)\,[\chi_n(m_2kR_1)/\psi_n(m_2kR_1)] - m_2[\chi_n'(m_2kR_1)/\psi_n(m_2kR_1)]}, \tag{4f}$$

where R_1 and R_2 are the radii for the core and the shell of the coated sphere, as is shown in Fig. 1, and D_n is the logarithmic derivative of the Riccati–Bessel function ψ_n, that is, $D_n(x) = \mathrm{d}[\ln \psi_n(x)]/\mathrm{d}x$. The coefficients a_n and b_n cannot be computed by use of a relative refractive index along with a scaled wavelength if m_0 is complex. In the case when the refractive index m_0 is unity, the coefficients in Eqs. (4a) and (4b) reduce to a form that is exactly identical to that given in Bohren and Huffman.[5] If the sphere is homogeneous, i.e., $m_2 = m_1$, the coefficients a_n and b_n reduce to the form

$$a_n = \frac{[m_0D_n(m_0kR)/m_1 + n/(m_0kR)]\psi_n(m_0kR) - \psi_{n-1}(m_0kR)}{[m_0D_n(m_0kR)/m_1 + n/(m_0kR)]\xi_n(m_0kR) - \xi_{n-1}(m_0kR)}, \tag{5a}$$

$$b_n = \frac{[m_1D_n(m_1kR)/m_0 + n/(m_0kR)]\psi_n(m_0kR) - \psi_{n-1}(m_0kR)}{[m_1D_n(m_1kR)/m_0 + n/(m_0kR)]\xi_n(m_0kR) - \xi_{n-1}(m_0kR)}, \tag{5b}$$

where R is the radius of the homogeneous sphere. The coefficients in Eqs. (5a) and (5b) are equivalent to the form presented in Kerker[3] and Ross[13] and that were recaptured in Fu and Sun.[12] Note that the form expressed by Eqs. (5a) and (5b) is more suitable for numerical computation, as is evident from the extensive discussions in Wiscombe[4] and Bohren and Huffman.[5] In the numerical computation of Eqs. (4a)–(4f), we took advantage of the various numerical techniques suggested by Wiscombe,[4,7] Bohren and Huffman,[5] and Toon and Ackerman.[8] In particular, following Kattawar and Hood,[14] in the computation of the higher-order terms of a_n and b_n in Eqs. (4a) and (4b) for large size parameters, we use the corresponding expressions in the homogeneous case for the two coefficients when $n > |m_1kR_1|$ to preserve numerical significance and also for computational economy.

B. Scattering Phase Matrix and Inherent and Apparent Cross Sections

For an incident wave propagating in an absorbing medium along the z axis of the coordinate system, the incident irradiance (i.e., the magnitude of the Poynting vector) can be written as follows:

$$F(z) = \left| \frac{c}{8\pi} \mathrm{Re}(\mathbf{E}_i \times \mathbf{H}_i^*) \right| = F_0 \exp(-2m_{0,i}kz), \tag{6}$$

where the asterisk indicates a complex conjugate and $m_{0,i}$ is the imaginary part of the refractive index of the host medium. The quantity F_0 is the incident irradiance at the origin of the coordinate system in the case when the scattering particle does not exist, which, derived on the basis of Eqs. (1a) and (1b), is equal to $cm_{0,r}|E_0|^2/(8\pi)$ where $m_{0,r}$ is the real part of the refractive index of the host medium. Note that $(c/8\pi)\mathrm{Re}(\mathbf{E}_i \times \mathbf{H}_i^*)$ in Eq. (6) is the time-averaged Poynting vector in the Gaussian unit system for a time-harmonic electromagnetic wave. Because the incident irradiance varies with the coordinate value z in the host medium, the definitions of various optical cross sections (i.e., the ratio of corresponding flux to the incident irradiance value at a reference location) are arbitrary in this case. That is, the cross sections depend on the selection of the reference incident irradiance plane. In the present study, we select the reference plane through the origin for the incident irradiance because of the advantage of this convention for application to multiple-scattering processes as we show in subsection 2.c. Thus the interception cross section of the particle for blocking the incident radiation, when it is defined with respect to the incident irradiance at the origin (i.e., the ratio of the incident flux intercepted by the particle to F_0), is then given by

$$\sigma_i = \frac{1}{F_0}\int_0^{2\pi}\int_{\pi/2}^{\pi} F(R_2\cos\theta)R_2^2\sin\theta\,\mathrm{d}\theta\mathrm{d}\phi = \pi R_2^2\,\frac{2[(2m_{0i}kR_2 - 1)\exp(2m_{0i}kR_2) + 1]}{(2m_{0i}kR_2)^2}. \tag{7}$$

Note that the expression of the total incident radiation flux intercepted by a sphere in an absorbing medium has been given by Mundy *et al.*[9] Evidently, the interception cross section depends not only on the particle geometric projected area but also on the dielectric properties of the host medium as well as on the incident wave number.

The total energy scattered by the particle, prior to its attenuation that is due to the absorption by the host medium, can be obtained when we integrate the radial component of the Poynting vector associated with the scattered wave on the particle surface. Thus the corresponding inherent scattering cross section defined with respect to the reference irradiance F_0 can be given as follows:

$$\begin{aligned}\sigma_s &= \frac{1}{F_0}\int_0^{2\pi}\int_0^{\pi}\frac{c}{8\pi}\,\mathrm{Re}\{[\mathbf{E}_s(\phi,\,\theta,\,R_2)\\ &\quad\times\mathbf{H}_s{}^*(\phi,\,\theta,\,R_2)]\cdot\hat{r}\}R_2{}^2\sin\theta\,\mathrm{d}\theta\,\mathrm{d}\phi\\ &= \frac{1}{F_0}\int_0^{2\pi}\int_0^{\pi}\frac{c}{8\pi}\,\mathrm{Re}[E_{s\theta}(\phi,\,\theta,\,R_2)H_{s\phi}{}^*(\phi,\,\theta,\,R_2)\\ &\quad- E_{s\phi}(\phi,\,\theta,\,R_2)H_{s\theta}{}^*(\phi,\,\theta,\,R_2)]R_2{}^2\sin\theta\,\mathrm{d}\theta\,\mathrm{d}\phi\\ &= \frac{2\pi}{m_{0r}k^2}\,\mathrm{Im}\Bigg\{\frac{1}{m_0}\sum_{n=1}^{\infty}(2n+1)\\ &\quad\times[|a_n|^2\,\xi_n{}'(m_0kR_2)\xi_n{}^*(m_0kR_2)\\ &\quad-|b_n|^2\,\xi_n(m_0kR_2)\xi_n{}'^*(m_0kR_2)]\Bigg\},\end{aligned}\tag{8}$$

where $\hat{r}$ is a unit vector along the radial direction. The symbols Re{ } and Im{ } indicate the real and imaginary parts of an argument, respectively. Similarly, the absorption cross section defined with respect to F_0 can be obtained as follows:

$$\begin{aligned}\sigma_a &= -\frac{1}{F_0}\int_0^{2\pi}\int_0^{\pi}\frac{c}{8\pi}\,\mathrm{Re}\{[\mathbf{E}_i(\phi,\,\theta,\,R_2)\\ &\quad+\mathbf{E}_s\,(\phi,\,\theta,\,R_2)]\times[\mathbf{H}_i{}^*(\phi,\,\theta,\,R_2)\\ &\quad+\mathbf{H}_s{}^*(\phi,\,\theta,\,R_2)]\cdot\hat{r}\}R_2{}^2\sin\theta\,\mathrm{d}\theta\,\mathrm{d}\phi\\ &= -\frac{1}{F_0}\int_0^{2\pi}\int_0^{\pi}\frac{c}{8\pi}\,\mathrm{Re}\{[E_{i\theta}(\phi,\,\theta,\,R_2)\\ &\quad+E_{s\theta}(\phi,\,\theta,\,R_2)]\cdot[H_{i\phi}{}^*(\phi,\,\theta,\,R_2)\\ &\quad+H_{s\phi}{}^*(\phi,\,\theta,\,R_2)]-[E_{i\phi}(\phi,\,\theta,\,R)\\ &\quad+E_{s\phi}(\phi,\,\theta,\,R_2)]\cdot[H_{i\theta}{}^*(\phi,\,\theta,\,R_2)\\ &\quad+H_{s\theta}{}^*(\phi,\,\theta,\,R_2)]\}R_2{}^2\sin\theta\,\mathrm{d}\theta\,\mathrm{d}\phi\\ &= \frac{2\pi}{m_{0r}k^2}\,\mathrm{Im}\Bigg\{\frac{1}{m_0}\sum_{n=1}^{\infty}(2n+1)\,[\psi_n(m_0kR_2)\psi_n{}'^*\\ &\quad\times(m_0kR_2)-\psi_n{}'(m_0kR_2)\psi_n{}^*(m_0kR_2)\\ &\quad+a_n\xi_n{}'(m_0kR_2)\psi_n{}^*(m_0kR_2)\\ &\quad-b_n\xi_n{}'(m_0kR_2)\psi_n{}'(m_0kR_2)\\ &\quad+a_n{}^*\psi_n{}'(m_0kR_2)\xi_n{}^*(m_1kR)\\ &\quad-b_n{}^*\psi_n(m_0kR_2)\xi_n{}'^*(m_0kR_2)\\ &\quad-|a_n|^2\,\xi_n{}'(m_0kR_2)\xi_n{}^*(m_0kR_2)\\ &\quad+|b_n|^2\,\xi_n(m_0kR_2)\xi_n{}'^*(m_0kR_2)]\Bigg\}.\end{aligned}\tag{9}$$

The extinction cross section σ_e corresponding to the scattering and absorption cross sections in Eqs. (8) and (9)—as is its conventional definition when the host medium is nonabsorptive—is the summation of the absorption and scattering cross sections, that is

$$\sigma_e = \sigma_a + \sigma_s. \tag{10}$$

Note that mathematical expressions that are similar to Eqs. (8) and (9) but in terms of absorbed and scattered energy have been presented by Sudiarta and Chylek[11] in the case for a homogeneous sphere. To derive the energy absorbed by a homogeneous sphere in an absorbing medium, Fu and Sun[12] used the internal field on the particle surface that is approached from the inside of the particle. It should be pointed out that the approach based on the internal field is more complicated than that based on the field outside the particle in the case for a coated sphere. The increased complexity occurs because the internal field for a coated sphere, as is shown in Bohren and Huffman,[5] is in the form of

$$\mathbf{E}_t = \sum_{n=1}^{\infty}E_n[f_n\mathbf{M}_{o1n}^{(1)} - ig_n\mathbf{N}_{e1n}^{(1)} + \nu_n\mathbf{M}_{o1n}^{(2)} - iw_n\mathbf{N}_{e1n}^{(2)}], \tag{11}$$

whereas the counterpart of the preceding expression in the case for a homogeneous sphere is in the form of

$$\mathbf{E}_t = \sum_{n=1}^{\infty}E_n[c_n\mathbf{M}_{o1n}^{(1)} - id_n\mathbf{N}_{e1n}^{(1)}]. \tag{12}$$

In Eqs. (11) and (12), $\mathbf{M}_{o,e1n}^{(1,2)}$ and $\mathbf{N}_{o,e1n}^{(1,2)}$ are vector spherical harmonics whose detailed definitions can be found in van de Hulst[2] and also in Bohren and Huffman.[5] We note that the numerical computation of the four coefficients in Eq. (11) is much more complicated than the computation of the two coefficients in Eq. (12).

We apply the conventional definitions of the scattering and extinction efficiencies to the cross sections given by Eqs. (8) and (10) and define formality efficiency factors as follows:

$$Q_e = \sigma_e/(\pi R_2{}^2), \tag{13a}$$

$$Q_s = \sigma_s/(\pi R_2{}^2). \tag{13b}$$

Furthermore, we introduce the interception efficiency that is defined as

$$Q_i = \sigma_i/(\pi R_2{}^2), \tag{14}$$

where σ_i is the interception cross section given by Eq. (7). It can be proven that the interception efficiency approaches to unity if the absorption of the host me-

dium reduces to zero. In this circumstance, the scattering and extinction efficiencies defined in Eqs. (13a) and (13b) regain their physical meanings as in the conventional sense. Note that the preceding efficiencies can be unbounded for a large size parameter if the host medium is strongly absorptive because the cross sections are specified with respect to the incident irradiance at the particle center, as is evident from Eqs. (7)–(10).

When the host medium is absorptive, the true or inherent scattering efficiency (hereafter referred to as $Q_{s,\mathrm{inh}}$) for the scattering particle should be defined as the ratio of the scattered energy to the incident energy intercepted by the particle. Similarly, the inherent extinction efficiency (hereafter referred to as $Q_{e,\mathrm{inh}}$) is the ratio of the total attenuated (scattered plus absorbed) energy to the portion of the incident energy intercepted by the particle. Mathematically, these two inherent optical efficiencies and their ratio (i.e., the inherent single-scattering albedo) can be expressed as follows:

$$Q_{e,\mathrm{inh}} = Q_e/Q_i, \tag{15a}$$

$$Q_{s,\mathrm{inh}} = Q_s/Q_i, \tag{15b}$$

$$\omega_{0,\mathrm{inh}} = Q_{s,\mathrm{inh}}/Q_{e,\mathrm{inh}} = Q_s/Q_e, \tag{15c}$$

where Q_e, Q_s, and Q_i are defined in Eqs. (13a), (13b), and (14), respectively. It is worth noting that the extinction and scattering efficiencies reported in Sudiarta and Chylek[11] and also in Fu and Sun[12] are the inherent quantities $Q_{e,\mathrm{inh}}$ and $Q_{s,\mathrm{inh}}$, defined in Eqs. (15a) and (15b). Evidently, the inherent efficiencies do not have the conventional meanings in that the corresponding cross sections are not the products of the efficiencies and the geometric projected area of the sphere. As a matter of fact, one can neither define extinction nor scattering cross section without properly referencing a location for the incident irradiance when the host medium is absorptive.

The preceding inherent scattering efficiency is derived from the near field at the particle surface and is less useful in practice because the scattered wave in the radiation zone is usually the relevant quantity. Thus it is necessary to derive the apparent optical properties based on the far-field information. Using Eqs. (2e) and (2f) and the asymptotic form of the Riccati–Bessel functions, we can obtain the scattered field in the radiation zone (or far field) that is given as follows:

$$E_{s\theta}(\phi, \theta, r)|_{|m_0 kr|\to\infty} = \cos\phi \frac{\exp(im_0 kr)}{-im_0 kr} E_0 S_2, \tag{16a}$$

$$E_{s\phi}(\phi, \theta, r)|_{|m_0 kr|\to\infty} = -\sin\phi \frac{\exp(im_0 kr)}{-im_0 kr} E_0 S_1, \tag{16b}$$

where the amplitude scattering functions S_1 and S_2 are given, respectively, by

$$S_1 = \sum_{n=1}^{\infty} \frac{2n+1}{n(n+1)} [a_n \pi_n(\cos\theta) + b_n \tau_n(\cos\theta)], \tag{16c}$$

$$S_2 = \sum_{n=1}^{\infty} \frac{2n+1}{n(n+1)} [a_n \tau_n(\cos\theta) + b_n \pi_n(\cos\theta)]. \tag{16d}$$

Equations, (16a) and (16b) are similar to their counterparts for the case when the host medium is nonabsorptive, except that the wave number in these expressions is scaled by the complex refractive index m_0. From Eqs. (16a) and (16b), the two components of the scattered wave that are parallel and perpendicular, respectively, to the scattering plane can be expressed in a matrix form as follows:

$$\begin{bmatrix} E_{s\parallel}(\phi, \theta, r) \\ E_{s\perp}(\phi, \theta, r) \end{bmatrix} = \frac{\exp(im_0 kr)}{-im_0 kr} \begin{bmatrix} S_2 & 0 \\ 0 & S_1 \end{bmatrix} \begin{bmatrix} E_{i0\parallel} \\ E_{i0\perp} \end{bmatrix}, \tag{17}$$

where $(E_{s\parallel}, E_{s\perp}) = (E_{s\theta}, -E_{s\phi})$ and $(E_{i0\parallel}, E_{i0\perp}) = (E_0 \cos\phi, E_0 \sin\phi)$. As the scattered wave in the far-field region is a transverse wave, the magnetic field can be related to the corresponding electric field by an expression similar to Eq. (1b). Thus the irradiance associated with the scattered wave in the radiation zone or the far-field region is given by

$$\begin{aligned} F_s(\phi, \theta, r) &= \frac{cm_{0,r}}{8\pi} (|E_{s,\parallel}|^2 + |E_{s,\perp}|^2) \\ &= \frac{cm_{0,r}}{8\pi} |E_0|^2 \frac{\exp(-2m_{0,i}kr)}{|m_0|^2 k^2 r^2} (|S_1|^2 + |S_2|^2) \\ &= \exp[-2m_{0,i}k(r - R_2)] F_0 \\ &\quad \times \frac{\exp(-2m_{0,i}kR_2)}{|m_0|^2 k^2 r^2} (|S_1|^2 + |S_2|^2). \end{aligned} \tag{18}$$

In Eq. (18), the factor $\exp[-2m_{1i}k(r - R_2)]$ accounts for the absorption of the host medium in the region between the particle and the observational point. The apparent scattering cross section of the particle, with respect to reference irradiance F_0, after it is traced back from the far-field scattered wave observed at a distance r from the origin of the coordinate system, with an associated correction of the wave attenuation that is due to the absorption effect of the host medium, is given by

$$\begin{aligned} \tilde{\sigma}_s &= \frac{\exp[2m_{0i}k(r - R_2)]}{F_0} \\ &\quad \times \int_0^{2\pi} \int_0^{\pi} F_s(\phi, \theta, r) r^2 \sin\theta \, d\theta \, d\phi \\ &= \frac{\exp(-2m_{0i}kR_2)}{|m_0|^2 k^2} \int_0^{2\pi} \int_0^{\pi} (|S_1|^2 \\ &\quad + |S_2|^2) \sin\theta \, d\theta \, d\phi = \frac{2\pi \exp(-2m_{0i}kR_2)}{|m_0|^2 k^2} \\ &\quad \times \sum_{n=1}^{\infty} (2n+1) (|a_n|^2 + |b_n|^2). \end{aligned} \tag{19}$$

A comparison of the scattering cross section in Eq. (19) with its counterpart in the case of a nonabsorptive host medium shows that they are similar except for an exponential factor $\exp(-2m_{0i}kR_2)$ along with a complex host medium refractive index m_0 involved in Eq. (19). Furthermore, the apparent scattering efficiency is quite different from its inherent counterpart, as is evident from the comparison between Eqs. (8) and (19). This discrepancy occurs because the host absorption over the distance between the particle and an observational point in the radiation zone cannot be accounted for exactly by the exponential factor $\exp[2m_{0i}k(r - R_2)]$. The local plane-wave feature of the scattered wave, described by the exponential form for the spatial phase variation in Eq. (17), is valid only for the far-field regime. Thus an assumption of exponential attenuation for the near-field region will overestimate or underestimate the absorption in the host medium. But this will not affect the multiple-scattering calculation as long as the apparent scattering cross section is used, although the host absorption is assumed to have an exponential form regardless of the location in the medium with respect to scattering particles.

In practice, it is critical to transform the incident Stokes vector to its scattered counterpart by use of the apparent single-scattering properties. On the basis of Eqs. (17) and (19) and the definition of the Stokes vector,[2] the Stokes vector associated with the scattered field is related to its incident counterpart through the scattering phase matrix as follows:

$$\begin{bmatrix} I_s(\phi, \theta, r) \\ Q_s(\phi, \theta, r) \\ U_s(\phi, \theta, r) \\ V_s(\phi, \theta, r) \end{bmatrix} = \frac{\exp[-2m_{0i}k(r - R_2)]\tilde{\sigma}_s}{r^2} \times \frac{P_{11}}{4\pi} \begin{bmatrix} 1 & P_{12}/P_{11} & 0 & 0 \\ P_{12}/P_{11} & 1 & 0 & 0 \\ 0 & 0 & P_{33}/P_{11} & -P_{33}/P_{11} \\ 0 & 0 & P_{43}/P_{11} & P_{33}/P_{11} \end{bmatrix} \begin{bmatrix} I_{i0} \\ Q_{i0} \\ U_{i0} \\ V_{i0} \end{bmatrix}, \tag{20}$$

where $[I_{i0}, Q_{i0}, U_{i0}, V_{i0}]$ is the incident Stokes vector at the origin of the coordinate system. Note that the incident Stokes vector associated with a wave propagating along the z coordinate axis can be expressed for an arbitrary location (ϕ, θ, r) in the form of

$$\begin{bmatrix} I_i(\phi, \theta, r) \\ Q_i(\phi, \theta, r) \\ U_i(\phi, \theta, r) \\ V_i(\phi, \theta, r) \end{bmatrix} = \exp(-2m_{0i}kr \cos\theta) \begin{bmatrix} I_{i0} \\ Q_{i0} \\ U_{i0} \\ V_{i0} \end{bmatrix}. \tag{21}$$

In Eq. (20) P_{11} is the normalized phase function in the sense that $[\int_0^\pi P_{11}(\cos\theta)\sin\theta d\theta]/2$ is unity. From the far-field perspective, the parameter $\tilde{\sigma}_s$ is the scattering cross section. For this reason, we refer to $\tilde{\sigma}_s$ as the apparent scattering cross section as viewed from a point away from the particle. The apparent scattering cross section should be used in any radiative transfer calculations dealing with the far field. The nonzero elements of the phase matrix in Eq. (21) take the same form as for the case for the nonabsorbing host medium and are given by

$$P_{11} = \frac{|S_1|^2 + |S_2|^2}{\sum_{n=1}^{\infty} (2n + 1)(|a_n|^2 + |b_n|^2)}, \tag{22a}$$

$$P_{12}/P_{11} = \frac{|S_2|^2 - |S_1|^2}{|S_2|^2 + |S_1|^2}, \tag{22b}$$

$$P_{33}/P_{11} = \frac{2\mathrm{Re}(S_1S_2^*)}{|S_2|^2 + |S_1|^{2\prime}}, \tag{22c}$$

$$P_{43}/P_{11} = \frac{2\mathrm{Im}(S_1S_2^*)}{|S_2|^2 + |S_1|^2}. \tag{22d}$$

The asymmetry factor has the same form for either the absorptive or the nonabsorptive host medium, as is evident from the comparison of the results presented by Kerker[3] and Fu and Sun.[12] In addition, the asymmetry factor for a coated sphere can be expressed in the same form as that for a homogeneous sphere, given by

$$g = \frac{1}{2}\int_0^\pi P_{11}(\cos\theta)\cos\theta \sin\theta d\theta = \frac{2\sum_{n=2}^{\infty} \{\mathrm{Re}[(n - 1)(n + 1)(a_{n-1}a_n^* + b_{n-1}b_n^*)/n] + (2n - 1)/[(n - 1)n]\mathrm{Re}(a_{n-1}b_{n-1}^*)\}}{\sum_{n=1}^{\infty}(2n + 1)\ (|a_n|^2 + |b_n|^2)}, \tag{23}$$

For the absorption within the particle, we do not distinguish between the apparent and the inherent

features. Thus the apparent extinction cross section associated with the $\tilde{\sigma}_s$ can be defined as follows:

$$\tilde{\sigma}_e = \sigma_a + \tilde{\sigma}_s, \tag{24}$$

where the absorption cross section is that defined in Eq. (9). As is similar to the case for inherent optical properties, the apparent scattering and extinction efficiencies can be defined as follows:

$$\tilde{Q}_e = \tilde{\sigma}_e/(\pi R_2{}^2), \tag{25a}$$

$$\tilde{Q}_s = \tilde{\sigma}_s/(\pi R_2{}^2). \tag{25b}$$

The apparent extinction and scattering efficiencies as well as the single-scattering albedo that are defined with respect to the truly intercepted incident irradiance are given by

$$Q_{e,\mathrm{app}} = \tilde{Q}_e/Q_i, \tag{26a}$$

$$Q_{s,\mathrm{app}} = \tilde{Q}_s/Q_i, \tag{26b}$$

$$\omega_{0,\mathrm{app}} = Q_{s,\mathrm{app}}/Q_{e,\mathrm{app}} = \tilde{Q}_s/\tilde{Q}_e. \tag{26c}$$

The preceding apparent scattering efficiency is essentially the unattenuated scattering efficiency defined by Mundy *et al.*[9] in the case of a homogeneous sphere. However, the extinction efficiency defined by those authors can be smaller than the scattering efficiency. This shortcoming is overcome by the present definition of apparent extinction efficiency.

C. Proper Form of Single-Scattering Properties for Multiple Scattering by a Polydisperse Particle System within an Absorbing Medium

In this subsection we present the radiative transfer equation derived for a polydispersive system in an absorbing medium based on the apparent single-scattering properties. For simplicity without losing generality, we consider the scalar radiative transfer equation. That is, we do not account for the full Stokes vector but only the intensity of radiation. Thus, according to Eq. (20), for the scattering process associated with an individual particle with a radius R, we can express the scattered intensity as

$$I_s(\phi, \theta, r) = \frac{\exp[-2m_{0i}k(r - R)]\tilde{\sigma}_s}{r^2}\frac{P_{11}}{4\pi} I_{i0}, \tag{27}$$

where $\tilde{\sigma}_s$ is the apparent scattering cross section defined in Eq. (19). In Eq. (27) the transformation of incident intensity to the scattered intensity explicitly involves the particle size R. This is a shortcoming that prevents the applicability of Eq. (27) to the multiple-scattering processes involving a polydisperse particle system. To circumvent this disadvantage, we define the scaled apparent cross section as follows:

$$\tilde{\sigma}_{s,\mathrm{scaled}} = \exp(2m_0 kR)\tilde{\sigma}_s, \tag{28a}$$

and consequently the scaled extinction cross section by

$$\tilde{\sigma}_{e,\mathrm{scaled}} = \sigma_a + \tilde{\sigma}_{s,\mathrm{scaled}}. \tag{28b}$$

With these definitions, Eq. (27) can be simplified as follows:

$$I_s(\phi, \theta, r) = \frac{\exp(-2m_{0i}kr)\tilde{\sigma}_{s,\mathrm{scaled}}}{r^2}\frac{P_{11}}{4\pi} I_{i0}. \tag{29}$$

In Eq. (29) the incident intensity is specified at the center of the particle. Through use of the scaled scattering cross section, the absorption path for two subsequential scattering event processes is measured between the centers of the particles. This feature substantially simplifies the radiative transfer calculation in an absorbing medium.

For a polydisperse particle system, let us assume the volume-normalized concentration for the particle at a location within the host medium to locally be $N(\mathbf{s}, R)$, where R is the radius of the particle and $\mathbf{s}$ is the position vector. The extinction and scattering coefficients that are due to the effect of particle scattering and absorption as viewed from the far-field perspective, rather than the absorption of the host medium, can be given by the particle's scaled apparent scattering properties as follows:

$$\tilde{\beta}_{e,p}(\mathbf{s}) = \int_{R_{\min}}^{R_{\max}} \tilde{\sigma}_{e,\mathrm{scaled}}(\mathbf{s}, R)N(\mathbf{s}, R)\mathrm{d}R, \tag{30a}$$

$$\tilde{\beta}_{s,p}(\mathbf{s}) = \int_{R_{\min}}^{R_{\max}} \tilde{\sigma}_{s,\mathrm{scaled}}(\mathbf{s}, R)N(\mathbf{s}, R)\mathrm{d}R, \tag{30b}$$

where the subscript p indicates that the extinction and scattering coefficients are for particles. The quantity $N(\mathbf{s}, R)$ has units of number per volume per length and $\tilde{\sigma}_{e,\mathrm{scaled}}$ (also $\tilde{\sigma}_{s,\mathrm{scaled}}$) has units of area. Thus both $\tilde{\beta}_{e,p}(\mathbf{s})$ and $\tilde{\beta}_{s,p}(\mathbf{s})$ have units of inverse length.

In the present formulation we ignore the Rayleigh scattering by the molecules of the host medium for the sake of simplicity, which, in principle, can be treated in the same manner as that for particulate inclusions in the medium. The extinction coefficient for the host medium is due solely to the absorption of the medium and is given by

$$\beta_{e,\mathrm{host}}(\mathbf{s}) = 2m_{0i}(\mathbf{s})k. \tag{31}$$

On the basis of the fundamental principle of radiative transfer (e.g., Chandrasekhar[15]) and Eqs. (30) and (31), the radiative transfer equation for the multiple-scattering process occurring in an absorbing medium can then be written as follows:

$$(\hat{\Omega}\cdot\nabla)I(\hat{\Omega}, \mathbf{s}) = -[\beta_{e,p}(\mathbf{s}) + \beta_{e,\mathrm{host}}(\mathbf{s})]I(\hat{\Omega}, \mathbf{s}) + J(\hat{\Omega}, \mathbf{s}), \tag{32a}$$

where $\hat{\Omega}$ is a unit vector specifying the propagating direction of the radiation. The first term on the right-hand side of Eq. (32a) corresponds to the atten-

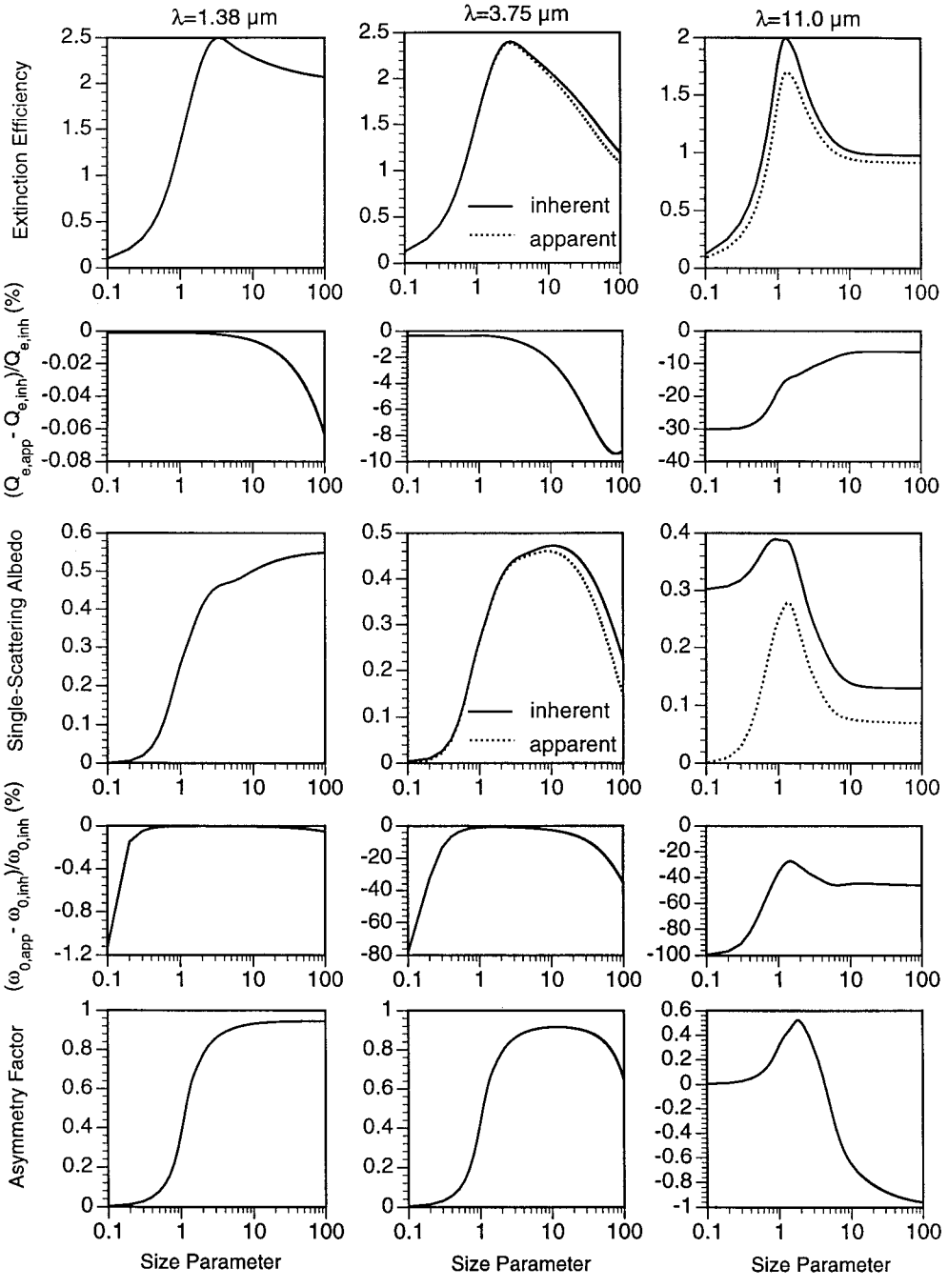

Fig. 2. Inherent and apparent extinction efficiency and single-scattering albedo values for soot spheres embedded in an ice medium at wavelengths of 1.38, 3.75, and 11.0 μm. Also shown are the asymmetry factor values.

uation of radiation by particle extinction and host medium absorption. $J(\hat{\Omega}, \mathbf{s})$ is the source function arising from the multiple scattering by the particles, given by

$$J(\hat{\Omega}, \mathbf{s}) = \frac{\hat{\beta}_{s,p}(\mathbf{s})}{4\pi} \int_{4\pi} I(\hat{\Omega}, \mathbf{s}) P_{11}(\mathbf{s}, \hat{\Omega}, \hat{\Omega}') \mathrm{d}\hat{\Omega}'. \quad (32b)$$

Table 1. Complex Refractive Index for Soot and Ice at Three Wavelengths[a]

Wavelength (μm)	Ice	Soot
1.38	$1.2943 + i1.580 \times 10^{-5}$	$1.7804 + i4.552 \times 10^{-1}$
3.75	$1.3913 + i6.796 \times 10^{-3}$	$1.9000 + i5.700 \times 10^{-1}$
11.0	$1.0925 + i2.480 \times 10^{-1}$	$2.23 + i7.300 \times 10^{-1}$

[a]Data are based on the interpolation of the data presented by Warren[19] and d'Almeida *et al.*[20] for ice and soot, respectively.

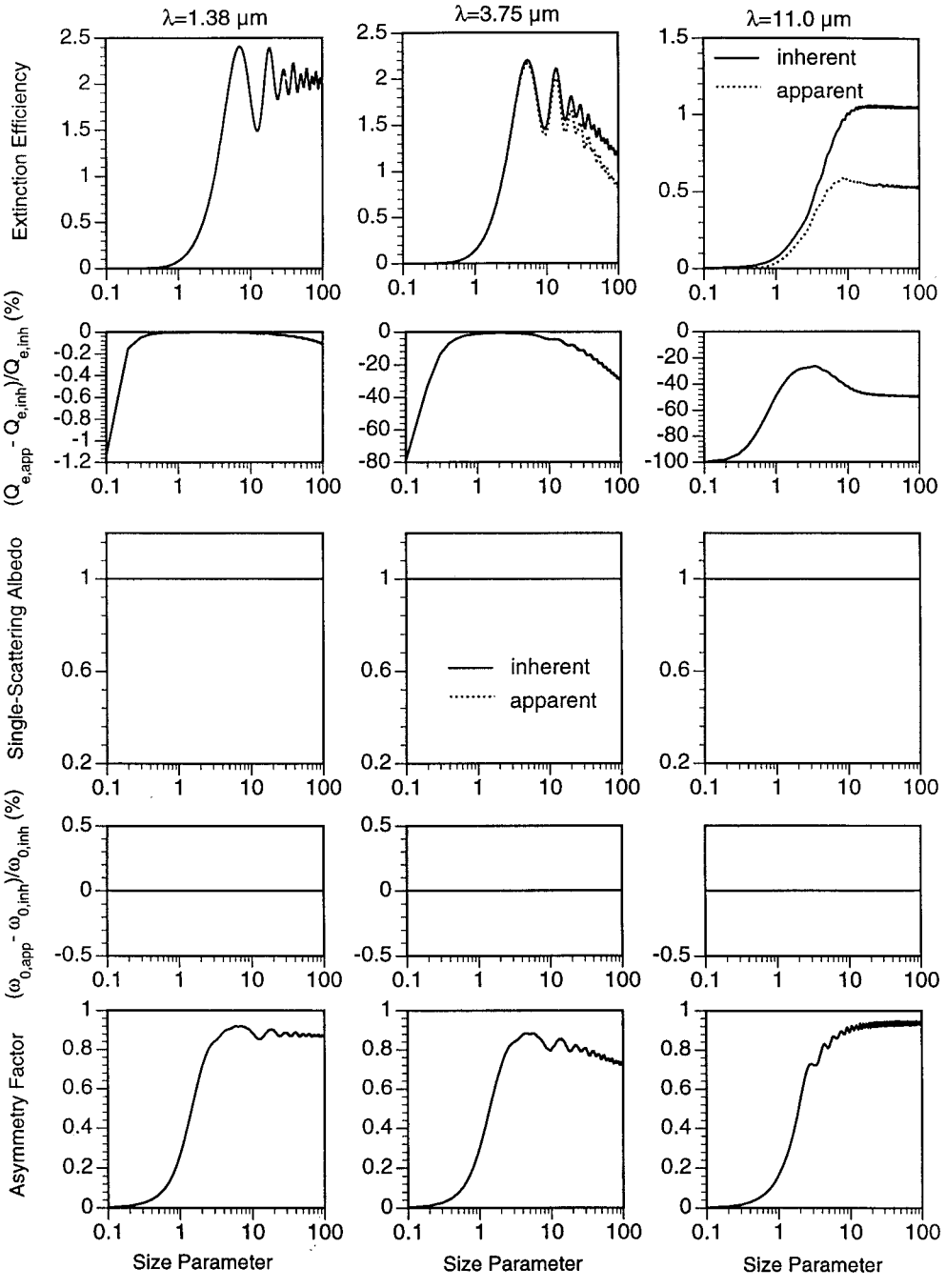

Fig. 3. Same as Fig. 2, except that the scatterers are air bubbles in an ice medium.

In Eqs. (32a) and (32b), we do not distinguish between the direct and diffuse radiation. In this form of the radiation transfer equation, the source of the radiation can be implemented through a boundary condition (e.g., Preisendorfer and Mobely[16]). In practice, numerical accuracy is achieved when we separate the diffuse and direct components of radiation. Situations exist where it is difficult to distinguish between the diffuse and the direct components of the radiation, such as for the solution of the radiation field inside a water layer with a wavy surface. In Eq. (32b), the phase function for the polydisperse system is given by the mean value obtained from the average particle phase function integrated over a specified particle size distribution and takes the form of

$$P_{11}(\mathbf{s}, \hat{\Omega}, \hat{\Omega}) = \frac{\int_{R_{\min}}^{R_{\max}} \tilde{\sigma}_{s,\,\mathrm{scaled}}(\mathbf{s}, R) P_{11}(\mathbf{s}, R, \hat{\Omega}, \hat{\Omega}) N(\mathbf{s}, R)\mathrm{d}R}{\int_{R_{\min}}^{R_{\max}} \tilde{\sigma}_{s,\,\mathrm{scaled}}(\mathbf{s}, R) N(\mathbf{s}, R)\mathrm{d}R}. \quad (33)$$

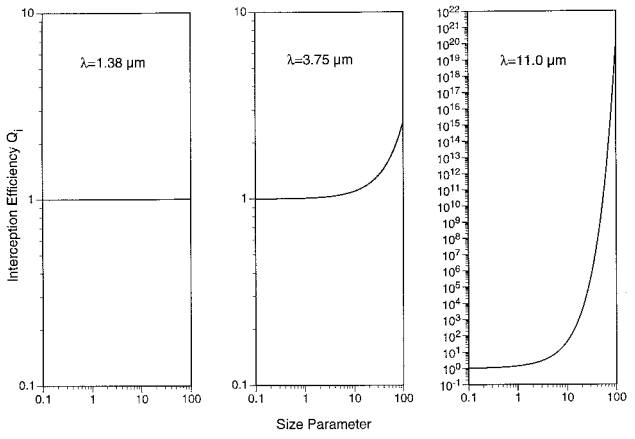

Fig. 4. Interception efficiency defined for particles embedded in an ice medium at three wavelengths.

It is straightforward to use the scaled apparent single-scattering properties in various radiative transfer computational methods, even for those that are not explicitly based on the radiative transfer equation. For example, in the Monte Carlo method involving an absorbing host medium, one can use $\tilde{\beta}_{e,p}(\mathbf{s})$ to determine the mean free path that a photon encounters in the next scattering or absorption event in the same manner as in the conventional method. For a scattering or absorption event, one can use the ratio of $\tilde{\beta}_{s,p}(\mathbf{s})$ to $\tilde{\beta}\eta_{e,p}(\mathbf{s})$ to determine whether the photon is scattered or absorbed. The new propagating direction of the scattered photon can be determined from the phase function according to a conventional algorithm. The effect of the absorption of the host medium is that the weight for the photon is scaled by a factor of $\exp(-2m_{0i}kd)$ between two successive scattering (or absorption) events, where d is the distance between the two events or, alternatively, the free path length. Furthermore, in dealing with multiple scattering in an absorptive host medium, weighting procedures for the bulk single-scattering properties may be a candidate for computational convenience (e.g., Tsay *et al.*[17], by Platnick and Valero[18]). Note that the emission contribution that normally exists for a strongly absorptive medium is not included in Eq. (32a) for simplicity, which, if included, could be treated in a manner similar to that discussed here.

3. Numerical Results and Discussion

On the basis the analyses in presented in Section 2, we developed a computational program to solve for the inherent and apparent optical efficiencies and the full phase matrix for a coated sphere within an absorbing medium. The previous codes written by Wiscombe,[4] Bohren and Huffman,[5] and Toon and Ackerman[8] for spheres in a nonabsorbing medium were of great benefit to the development of the present code. In particular, we find that the convergence criterion suggested by Wiscombe[4,7] is useful for computational efficiency and accuracy. The present code was validated by comparison with the previous inherent optical efficiencies and phase function of homogeneous spheres in an absorbing medium reported by Sudiarta and Chylek[11] and Fu and Sun.[12] In addition, the results obtained from the present code agree well with those from the conventional Lorenz–Mie calculations when the absorption of the host medium is reduced to zero.

Figure 2 shows the inherent and apparent extinction efficiency, single-scattering albedo, and asymmetry factor for spheres of soot embedded within ice at 1.38, 3.75, and 11 μm. The complex refractive indices of ice and soot at the three wavelengths are obtained by interpolation of Warren's data[19] for ice and d'Almeida *et al.*'s data[20] for soot and are listed in Table 1. These three wavelengths were chosen because they are commonly used in airborne or satellite retrieval. The 1.38-μm band is effective for the detection of cirrus clouds. The single-scattering properties of soot or air bubbles within ice are interesting to the study of cirrus clouds. Ice crystals within cirrus clouds may contain black carbon coming from biomass burning, which to our knowledge has not been fully explored. Furthermore, ice crystals may contain pockets of air bubbles; this effect has also been ignored to our knowledge in the computation of single-scattering properties. To solve for the optical properties of ice crystals with impurities on the basis of the ray-tracing technique (e.g., Macke *et al.*,[21] Labonnote *et al.*[22]), a Lorenz–Mie calculation is carried out for the inclusions that are assumed to be small, and the surrounding ice medium is treated as unbound.

From Fig. 2 the inherent and apparent values are essentially the same at 1.38 μm for both the extinction efficiency and the single-scattering albedo because the absorption of ice is negligible at this wavelength. However, substantial differences between the inherent and the apparent optical properties are noted at 3.75 and 11 μm, in particular, for the case of the single-scattering albedo at 11 μm. From Fig. 2, one can see that the apparent scattering cross section is smaller than its inherent counterpart. Figure 2 also presents the asymmetry factor for the phase function—note that the asymmetry factor can be negative. In addition, the inherent extinction efficiency converges to 1 instead of 2. These two features associated with the optical properties of a sphere in an absorbing medium have been reported by Sudiarta and Chylek[11] and Fu and Sun.[12]

Figure 3 is similar to Fig. 2, except that the scatter in the former case is a void (air bubble) in the medium. Because the air bubble is nonabsorbing, both the inherent and the apparent single-scattering albedos are unity. For the extinction efficiency, significant differences are evident from a comparison of the apparent and inherent optical properties at 3.7 and 11.0 μm, wavelengths at which ice is strongly absorptive. For the asymmetry factor shown in Fig. 3, negative values are not observed. When the host medium is strongly absorptive, the diffraction wave that contributes to forward scattering is essentially suppressed. If the scattering particle is also

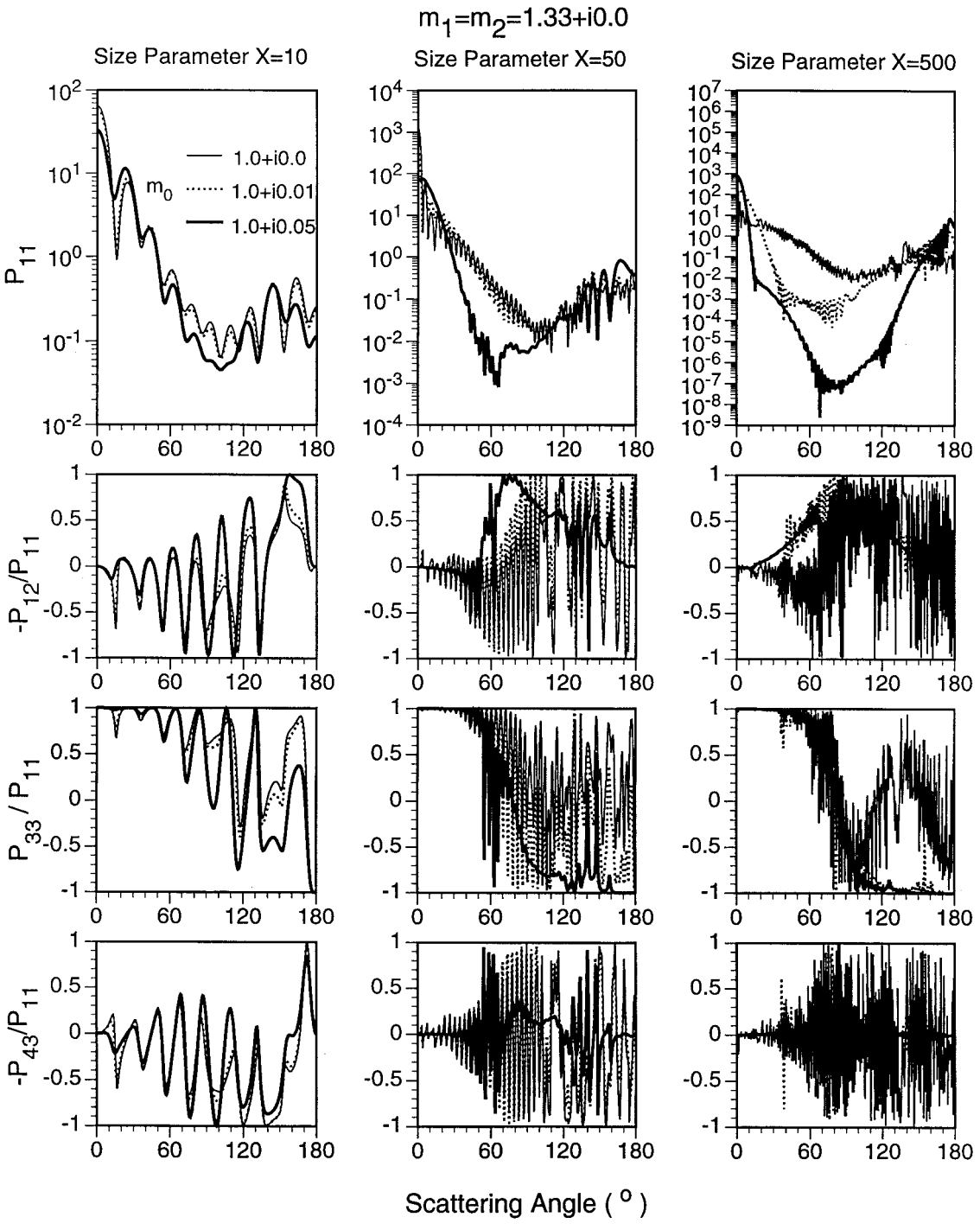

Fig. 5. Nonzero phase-matrix elements for homogeneous (uncoated) spheres that are embedded in an absorbing media. Results are provided for three values of the imaginary refractive index and for three size parameters. The particle refractive index is assumed to be 1.33 + i0.0, which is essentially the refractive index for water at a visible wavelength.

strongly absorptive, there is no transmittance through the particle to contribute to forward scattering. In this case the backscattering can be larger than the forward scattering, leading to a negative asymmetry factor. Contrary to this argument, for the air bubble case shown in Fig. 3, there still is a significant amount of radiation transmitted through the air bubble, and the forward scattering is stronger than the backscattering.

To convert the inherent or apparent extinction or scattering efficiency to the corresponding cross section, the interception efficiency factor Q_i is required, as is evident from Eqs. (15a)–(15b) and (26a)–(26b). Figure 4 shows the interception efficiency for three

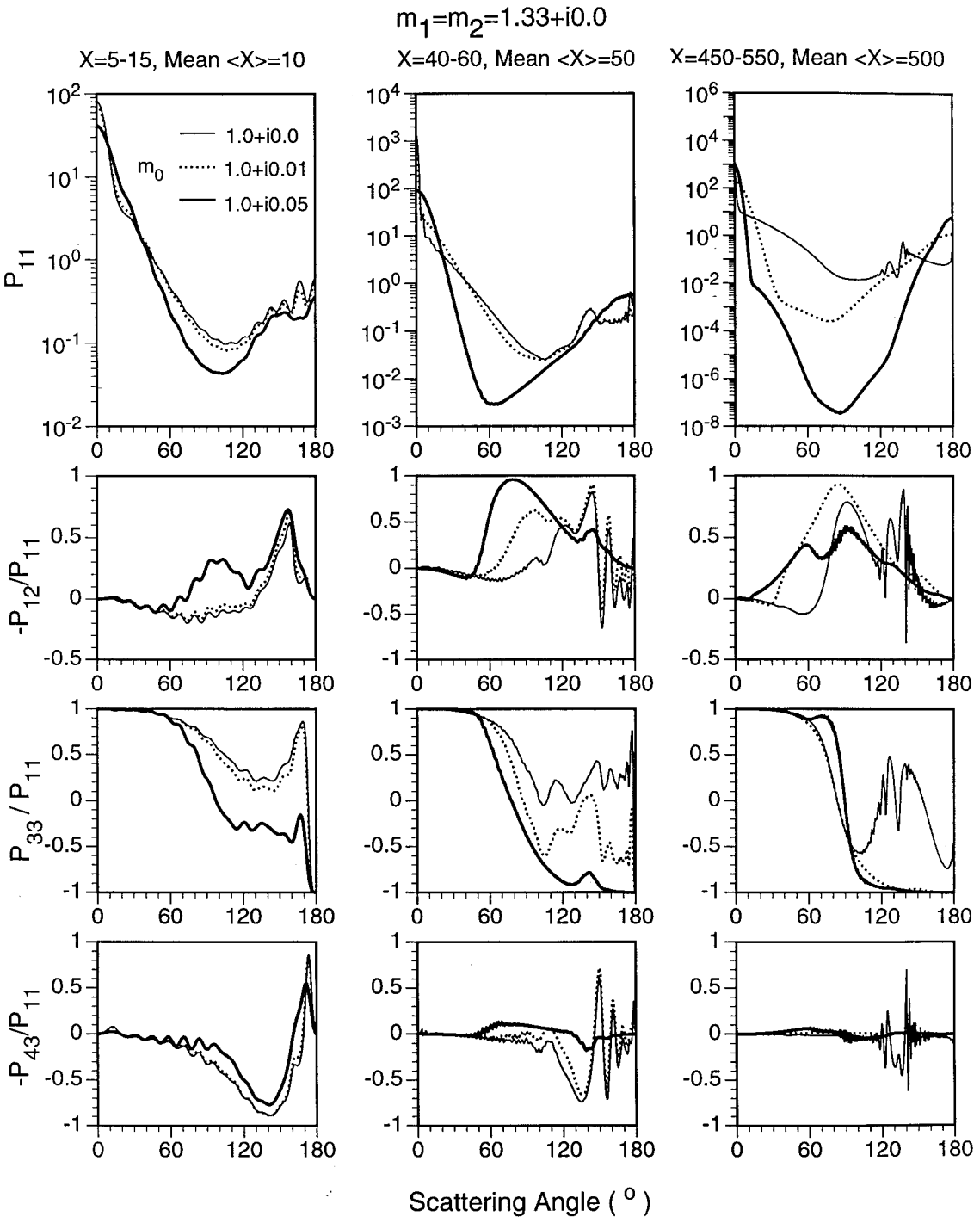

Fig. 6. Same as Fig. 5, except for a multidisperse particle system.

wavelengths with ice as the host medium. At the 1.38-μm wavelength, the absorption of ice is negligible, and Q_i is essentially unity. However, for the two absorbing wavelengths, the interception efficiency can be large. In particular, at 11 μm, the Q_i factor can be unbounded when the particle size increases. This occurs because the interception factor is defined with respect to the incident irradiance at the particle center. For a strongly absorptive host medium, the incident irradiance can be attenuated substantially within a distance of the order of the particle radius that is comparable to the incident wavelength.

Figure 5 shows the complete nonzero elements of a phase matrix for homogeneous spheres within an absorbing media. For the host medium, the refractive index is selected as $1.0 + i0.0$, $1.0 + i0.01$, and $1.0 + i0.05$, corresponding to the values used in Sudiarta and Chylek.[11] The particle refractive index is selected as $1.33 + i0.0$ that is essentially the refractive index of a water droplet at a visible wavelength. Ob-

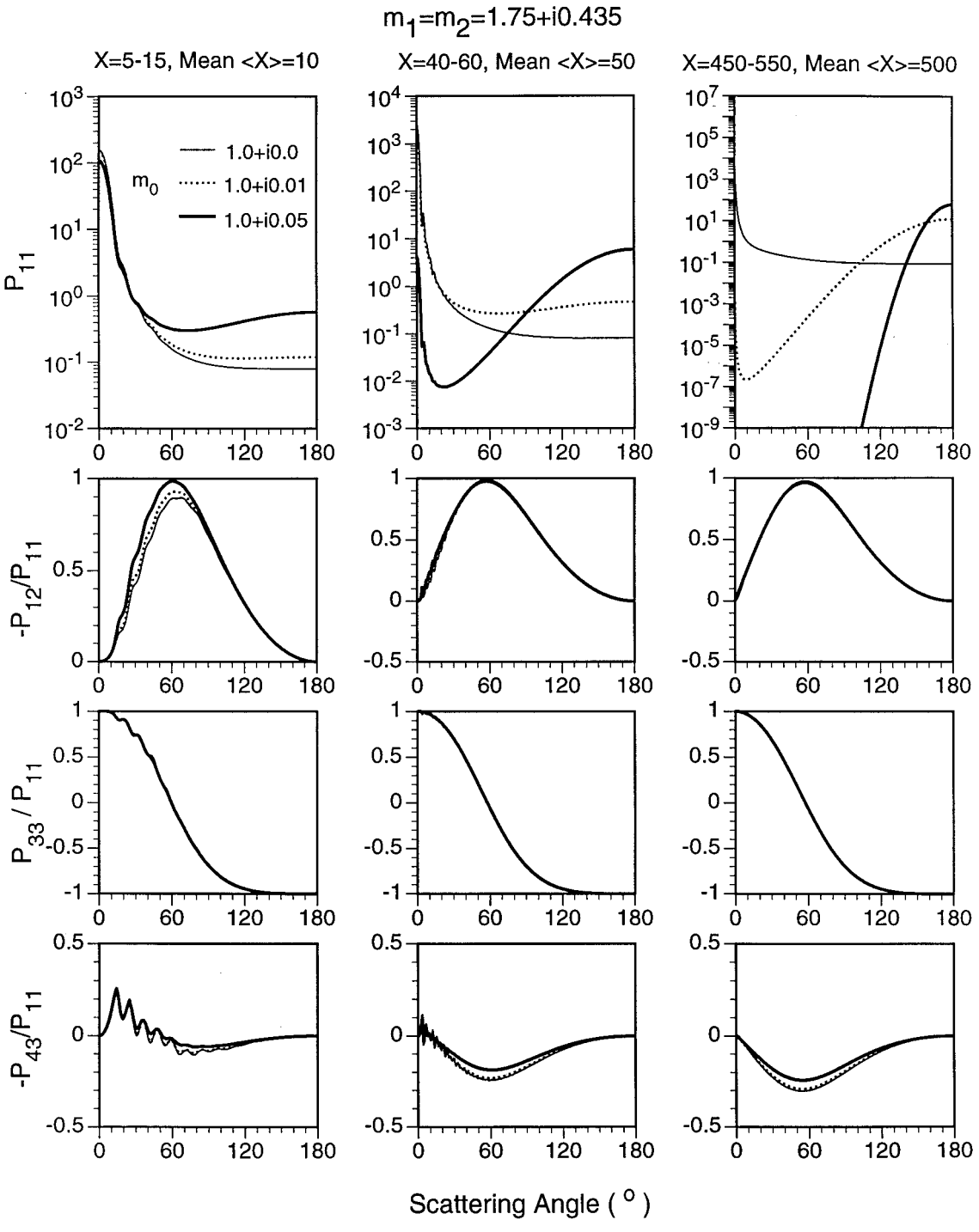

Fig. 7. Same as Fig. 6, except that the particle refractive index is 1.75 + i0.435, which is the refractive index for soot at a visible wavelength.

viously, the absorption of the host medium substantially influences the scattering phase matrix of the particles, particularly for the large size parameter. For the moderate size parameter $X = 50$ and large size parameter $X = 500$, the scattering of the sphere is substantially reduced in sidescattering directions when the host absorption is strong, as is evident from the phase functions shown. For scattering by an individual sphere, the resonant effect is significant for the phase-matrix elements associated with polarization. The resonant effect is particularly pronounced for the phase elements associated with the polarization configuration. Recently, using modern visualization techniques, Mishchenko and Lacis[23] investigated the morphology-dependent resonances for homogeneous spheres within a nonabsorbing host medium. In future research, it would be interesting to study the impact of the host ab-

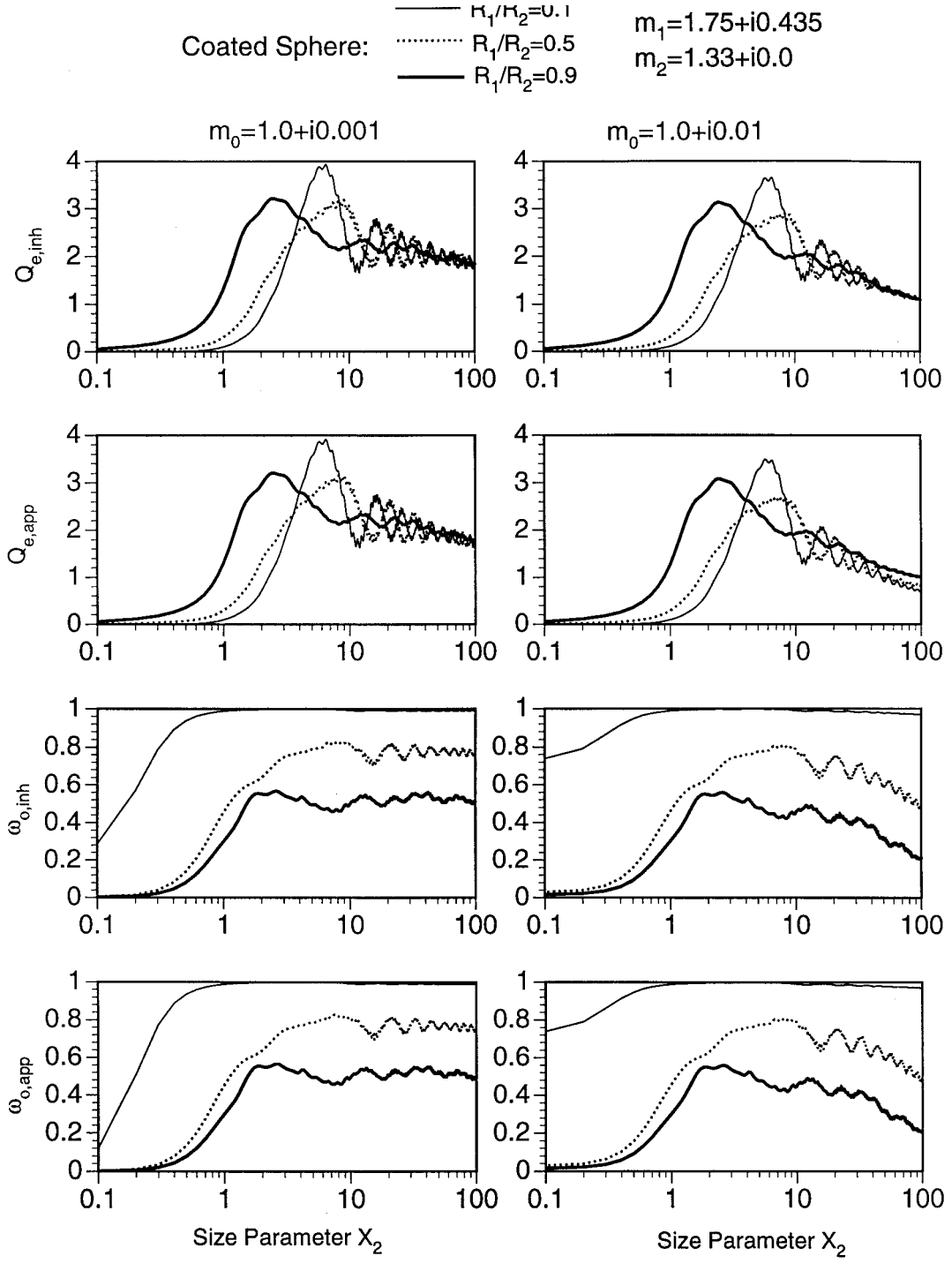

Fig. 8. Comparison of inherent and apparent extinction efficiency and single-scattering albedo for a soot sphere coated with water. The refractive indices for the host medium were chosen to be $1.0 + i0.001$ and $1.0 + i0.01$.

sorption on the resonances in a manner suggested by those authors.

To smooth out the resonant fluctuations, we include a size distribution in the scattering calculation. Figure 6 shows the phase matrix for three mean size parameters: 10 with a bin width of 5–15, 50 with a bin width of 40–60, and 500 with a bin width of 450–550. The effect of the host absorption is pronounced. For a strong absorbing host medium, the phase function value is significantly reduced in forward and sidescattering directions. In particular, the rainbow feature associated within a scattering by spheres is smoothed out by the host absorption, as can be seen from the phase functions shown for the case of $\langle X \rangle = 500$. The effect of the host absorption on the polarization configuration of the scattered wave is also evident, which is particularly significant for P_{33}/P_{11} and $-P_{12}/P_{11}$.

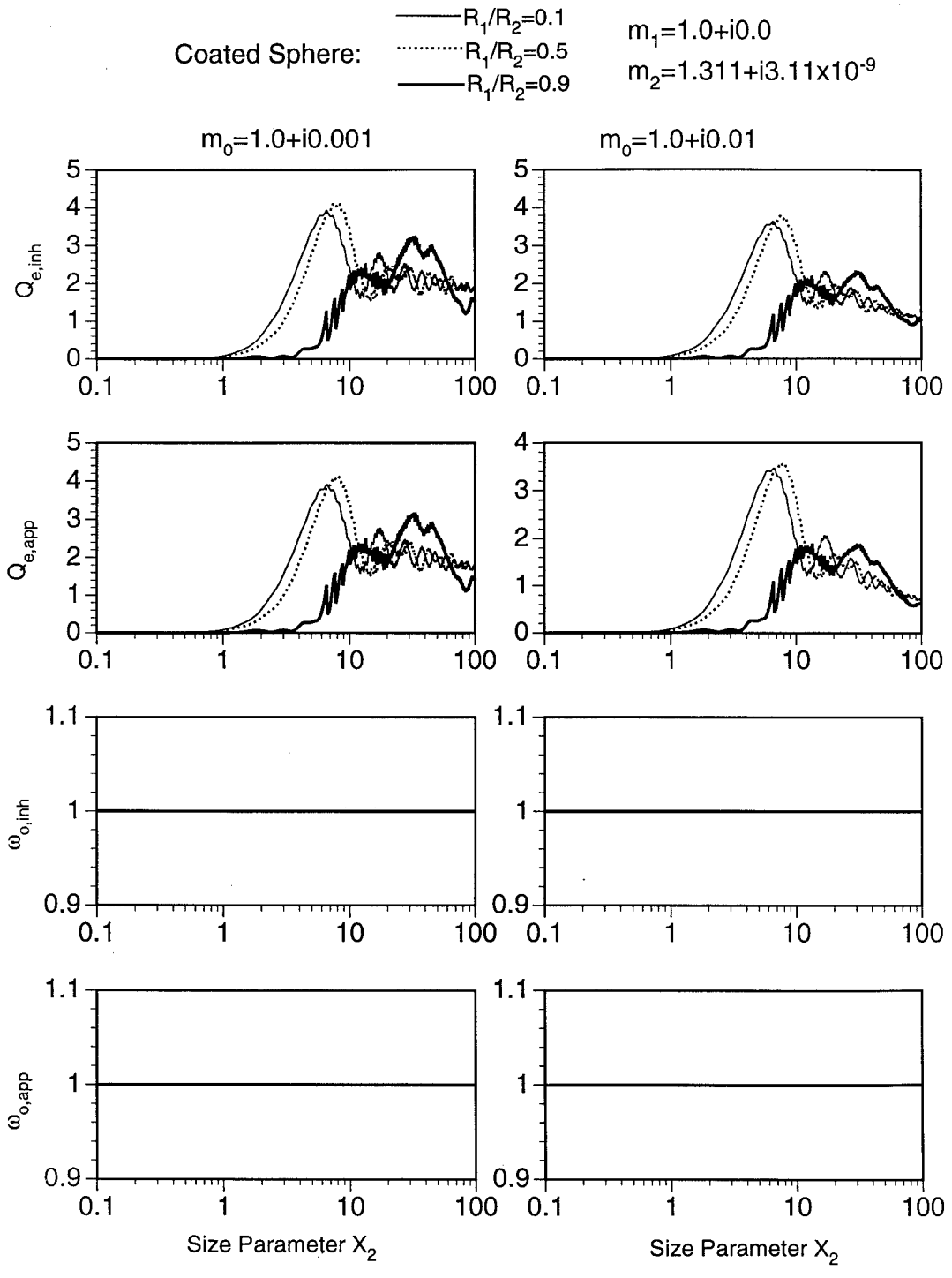

Fig. 9. Same as Fig. 8, except that the scattering particles are hollow ice spheres.

Figure 7 is similar to Fig. 6, except that the scattering particle is soot. For the moderate and large size parameters, i.e., $\langle X \rangle = 50$ and 500, the phase function values are larger for backscattering directions than for either forward or sidescattering directions when the host absorption is large. This occurs because soot is a strongly absorbing medium and does not allow the transmission of the incident radiation whereas the host absorption suppresses the diffraction peak. From Fig. 7, it can also be noted that the host absorption has a minor effect on polarization. Because soot is absorptive, the external reflection occurring at the particle surface dominates the scattered field. The polarization configuration of the externally reflected wave is not sensitive to particle size and the host absorption.

Black carbon in the atmosphere may serve as nuclei for cloud droplets and modifies the bulk radiative

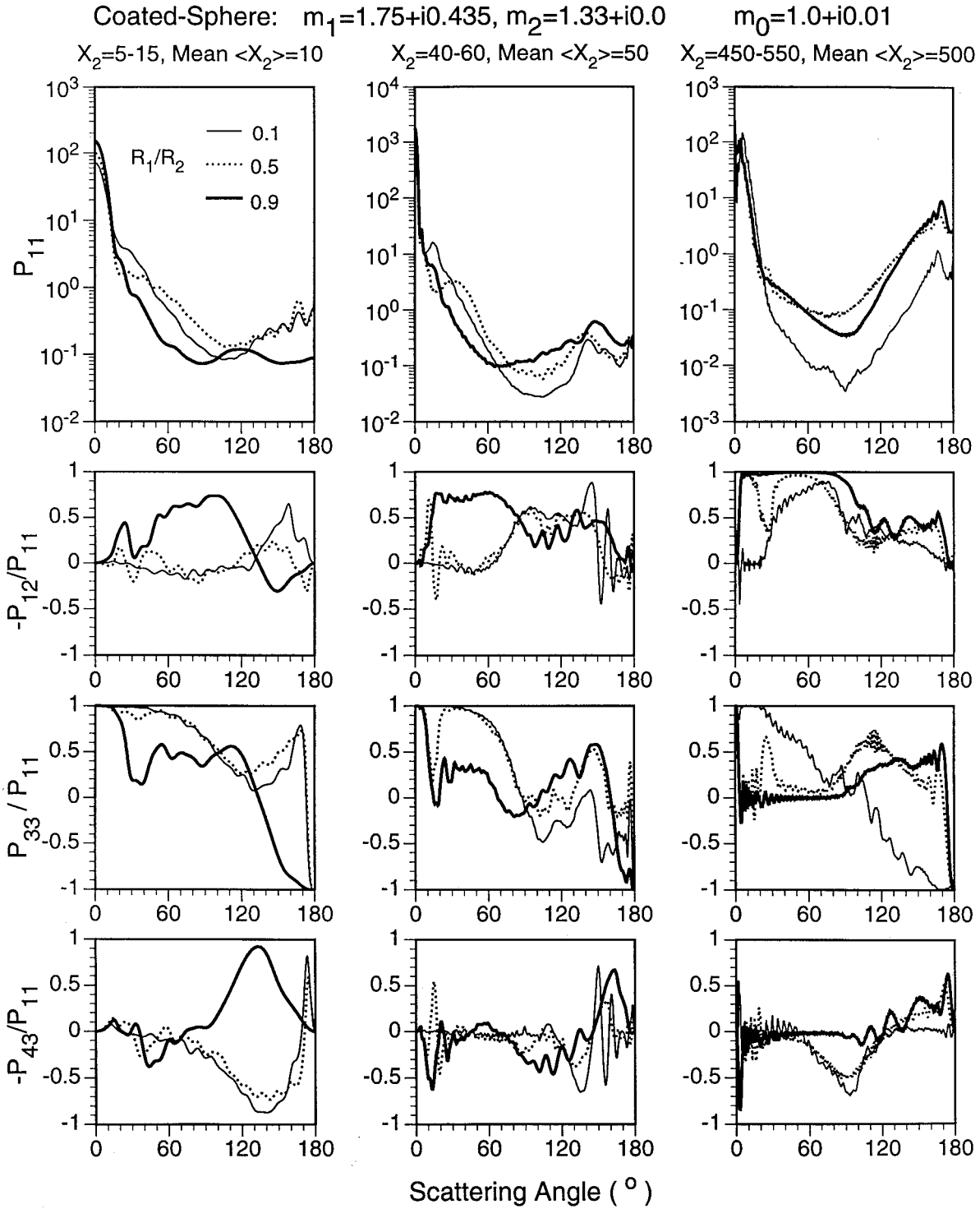

Fig. 10. Phase-matrix elements for a particle of water-coated soot. The host refractive index was chosen as $1.0 + i0.01$.

properties of clouds. Figure 8 shows the inherent and apparent extinction efficiency and single-scattering albedo for water droplets containing soot for weak and strong host absorption conditions. The ratio of the radius of the soot core to the radius of the water shell was selected as $R_1/R_2 = 0.1$, 0.5, and 0.9. For extinction efficiency, the effect of the impurity on water droplets is primarily in the size parameter region of 1–20 because the extinction efficiency will approach its asymptotic value when the size parameter is large. The effect of the impurity on single scattering, however, is pronounced for the entire size parameter spectrum shown. Even a small amount of soot added to water droplets can substantially reduce the single-scattering albedo, as is evident from the case for $R_1/R_2 = 0.1$. For weak host absorption

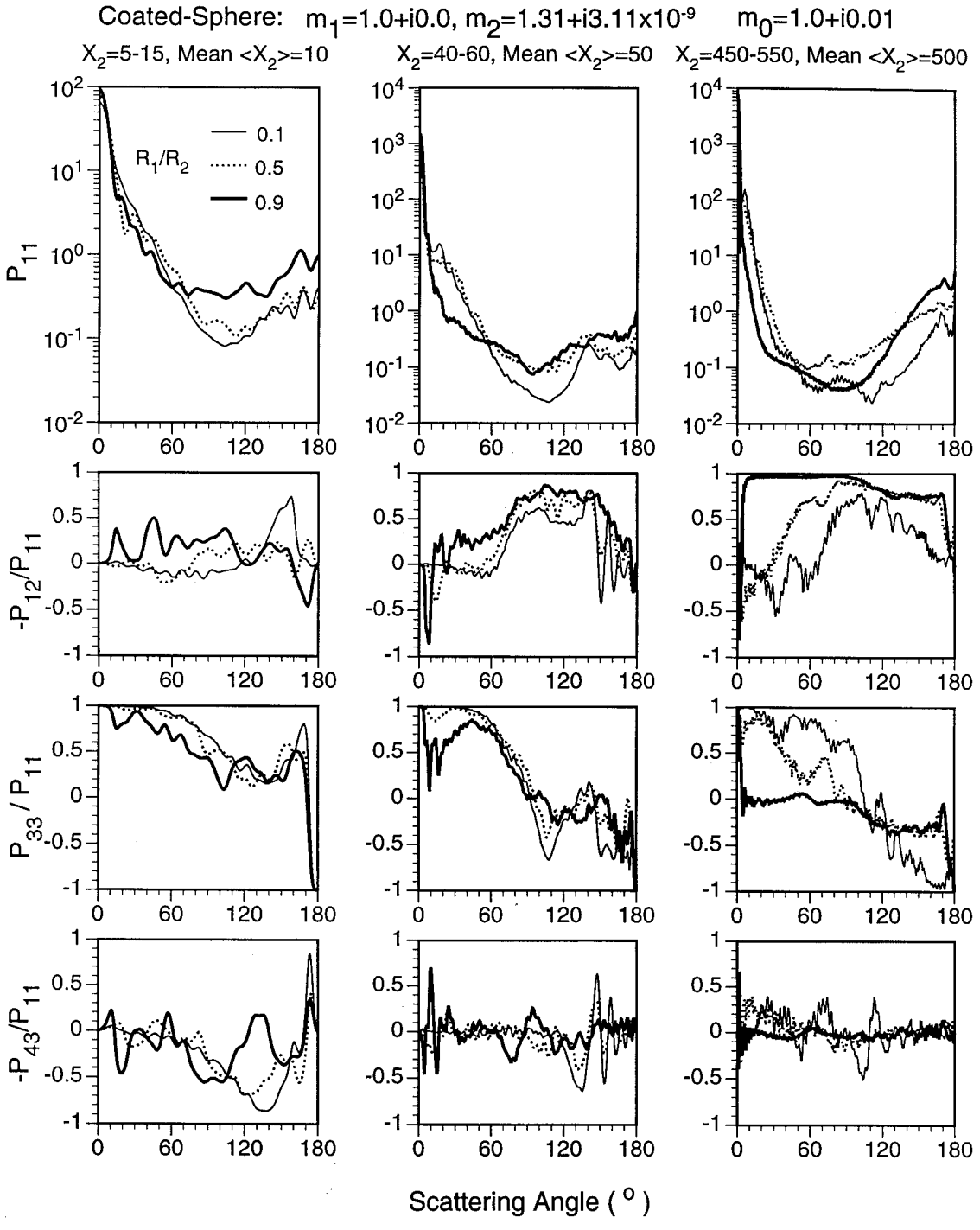

Fig. 11. Same as Fig. 10, except for a hollow ice sphere.

values, the single-scattering albedo tends to reach its asymptotic value when the size parameter is large. On the contrary, the single-scattering albedo decreases with increasing size parameter in the large size parameter regime if a strong host absorption is involved.

Figure 9 is similar to Fig. 8, except that Fig. 9 shows results for ice spheres containing air bubbles. Because the imaginary part of ice is small and the air bubble is nonabsorptive, both the inherent and the apparent single-scattering albedos are essentially unity regardless of the thickness of the ice shell of the particles. From the extinction efficiencies shown, the extinction maximum is shifted toward large size parameters when the thickness of the ice shell decreases. In addition, the host absorption reduces the asymptotic values of the extinction efficiency in a manner similar to the case for a homogeneous sphere.

Figures 10 and 11 show the nonzero elements of the phase matrix for soot spheres coated with a water

shell and for ice spheres containing air bubbles, respectively. For both cases, the refractive index of the host medium is assumed as $1.0 + i0.01$. A significant sensitivity to the ratio of the core size to the shell size is demonstrated for the single-scattering properties. For the coated black carbon, the polarization configuration for the case when black carbon is dominant (i.e., $R_1/R_2 = 0.9$) is quite different from the other two cases for which the water is the dominant component of the scatterer. Similarly, for the case of a hollow ice sphere, the polarization feature is unique when the ice shell is thin and the particle size is large.

4. Summary and Conclusions

We have extended the conventional Lorenz–Mie formalism to the scattering process associated with a coated sphere embedded within an absorbing medium. We have clarified that there are two ways to derive the scattering and extinction cross sections. The scattering cross section derived from the near field on the particle surface is the inherent optical properties of the particles, which is less useful in practice. Alternatively, the scattering cross section can be derived from the far-field wave with a proper scaling of the host medium absorption over the distance between the particle and the location where the far field is specified. This defines the apparent optical properties that implicitly contain the host absorption information in the near-field regime. We have shown that the mathematical expressions for the inherent and apparent scattering properties are quite different. Furthermore; we have developed a computational code to compute the inherent and apparent extinction efficiencies, single-scattering albedos, and asymmetry factors as well as the complete phase matrix.

Numerical calculations for spheres in absorbing media show that apparent and inherent optical properties can be different by several tens of percent if the host absorption is strong. The difference, however, reduces to zero if the host absorption is negligible. If the scattering particle is transparent (i.e., the imaginary part of the refractive index is zero), the host absorption has a significant impact on the nonzero elements of the phase matrix associated with the polarization configuration of the scattered wave. We find that the effect of the host absorption on the polarization effect is small if the particle itself is also strongly absorptive even if the host medium is substantially absorptive. Two specific applications discussed were of the scattering characteristics of (a) black carbon coated with water and (b) hollow ice spheres, i.e., ice spheres containing air bubbles. We found that black carbon included in water droplets can substantially reduce the single-scattering albedo for a small size parameter even if the amount of the impurity is small. For hollow ice spheres, the single-scattering albedo is essentially unity regardless of host absorption. However, the variation pattern of the extinction efficiency versus size parameter can be substantially changed by a strong host absorption.

In the case of a large size parameter ($\langle X \rangle = 500$) for coated soot or hollow ice spheres, the polarization elements of the phase matrix are unique in that $-P_{12}/P_{11}$ approaches unity whereas P_{33}/P_{11} reduces to zero for scattering angles between 10° and 80° if the particle shells are thin. Finally, we have defined a proper form of single-scattering properties for application to multiple-scattering computation. It was shown that the conventional technique for radiative transfer calculations can be applied if the scaled apparent single-scattering properties are used.

This research is supported by the NASA Radiation Sciences Program managed by Don Anderson and partially supported by the NASA moderate-resolution imaging spectroradiometer (MODIS), NASA Cloud-Aerosol Lidar and Infrared Pathfinder Satellite Observations (CALIPSO), the U.S. Office of Naval Research, the Multidisciplinary Research Program of the University Research Initiative (MURI) funded through the Navy Indian Ocean METOC Imaging (IOMI) mission for the Geostationary Imaging Fourier Transform Spectrometer (GIFTS), and the Atmospheric Radiation Measurement (ARM) Program under contract DE-AI02-00ER62901.

References

1. G. Mie, "Beigrade zur optik truber medien, speziell kolloidaler metallosungen," Ann. Phys. (Leipzig) **25,** 377–455 (1908).
2. H. C. van de Hulst, *Light Scattering by Small Particles* (Wiley, New York, 1957).
3. M. Kerker, *The Scattering of Light and Other Electromagnetic Radiation* (Academic, New York, 1963).
4. W. J. Wiscombe, "Mie scattering calculation," NCAR Tech. Note TN-140+STR (National Center for Atmospheric Research, Boulder, Colo., 1979).
5. C. F. Bohren, and D. R. Huffman, *Absorption and Scattering of Light by Small Particles* (Wiley, New York, 1983).
6. J. Dave, "Subroutines for computing the parameters of the electromagnetic radiation scattered by a sphere," IBM Rep. 320-3237 (IBM Scientific Center, Palo Alto, Calif., 1968).
7. W. J. Wiscombe, "Improved Mie scattering algorithms," Appl. Opt. **19,** 1505–1509 (1980).
8. O. B. Toon, and T. P. Ackerman, "Algorithms for the calculation of scattering by stratified spheres," Appl. Opt. **20,** 3657–3660 (1981).
9. W. C. Mundy, J. A. Roux, and A. M. Smith, "Mie scattering by spheres in an absorbing medium," J. Opt. Soc. Am. **64,** 1593–1597 (1974).
10. P. Chylek, "Light scattering by small particles in an absorbing medium," J. Opt. Soc. Am. **67,** 561–563 (1977).
11. I. W. Sudiarta, and P. Chylek, "Mie scattering formalism in absorbing medium," in the *Proceedings of the Fifth Conference on Light Scattering by Nonspherical Particles: Theory, Measurements, and Applications,* G. Videen, Q. Fu, and P. Chylek, eds. (U.S. Army Research Laboratory, Adelphi, Md., 2000), pp. 115–118.
12. Q. Fu, and W. Sun, "Mie theory for light scattering by a spherical particle in an absorbing medium," Appl. Opt. **40,** 1354–1361 (2001).
13. W. D. Ross, "Computation of Bessel functions in light scattering studies," Appl. Opt. **11,** 1919–1923 (1972).
14. G. W. Kattawar, and D. A. Hood, "Electromagnetic scattering

from a spherical polydispersion of coated spheres," Appl. Opt. **15,** 1996–1999 (1976).
15. S. Chandrasekhar, *Radiative Transfer* (Oxford U. Press, London, 1950).
16. R. W. Preisendorfer, and C. D. Mobely, "Direct and inverse irradiance models in hydrologic optics," Limnol. Oceanogr. **29,** 903–929 (1984).
17. S.-C. Tsay, K. Stamnes, and K. Jayaweera, "Radiative energy budget in the cloudy and hazy arctic," J. Atmos. Sci. **46,** 1002–1018 (1989).
18. S. Platnick and F. P. J. Valero, "A validation of a satellite cloud retrieval during ASTEX," J. Atmos. Sci. **15,** 2985–3001 (1995).
19. S. Warren, "Optical constants of ice from the ultraviolet to the microwave," Appl. Opt. **23,** 1206–1225 (1984).
20. G. A. d'Almeida, P. Koepke, and E. P. Shettle, *Atmospheric Aerosols: Global Climatology and Radiative Characteristics* (Deepak, Hampton, Va., 1991).
21. A. Macke, M. I. Mishchenko, and B. Cairns, "The influence of inclusions on light scattering by large ice particles," J. Geophys. Res. **101,** 23311–23316 (1996).
22. L. C. Labonnote, G. Brogniez, J.-C. Buriez, M. Doutriaux-Boucher, J. F. Gayet, and A. Macke, "Polarized light scattering by inhomogeneous hexagonal monocrystals: validation with ADEOS-POLDER measurements," J. Geophys. Res. **106,** 12139–12154 (2001).
23. M. I. Mishchenko, and A. A. Lacis, "Manifestations of morphology-dependent resonances in Mie scattering matrices," Appl. Math. Comput. **116,** 167–179 (2000).